AN ENTRY HANDBOOK FOR THE CONCEPTUAL DESIGN OF MARS MISSIONS

Grant Wells[(1)], Robert Braun[(2)]

[(1)]*Guggenheim School of Aerospace Engineering, Georgia Institute of Technology, Atlanta, Georgia, USA, Email: gtg315z@mail.gatech.edu*
[(2)]*Guggenheim School of Aerospace Engineering, Georgia Institute of Technology, Atlanta, Georgia, USA, Email: robert.braun@ae.gatech.edu*

ABSTRACT

The purpose of this investigation is to investigate trends in Mars entry, descent and landing conceptual mission design and propose a method of presenting this information as a handbook for conceptual design. The premise of the project is that Mars entry, descent and landing can be parameterized with five variables: (1) entry mass, (2) entry velocity, (3) entry flight path angle, (4) vehicle aeroshell diameter, and (5) vertical lift-to-drag ratio. For combinations of these input parameters, the following trajectory information will be determined: peak deceleration, peak heat rate, heat load, and the altitude at which Mach 2 is reached (for parachute deployment).

1. INTRODUCTION

A Mars entry, descent and landing (EDL) mission design handbook would serve as the initial basis for planetary probe EDL in the same manner that a Mars interplanetary mission design handbook serves as the initial basis for launch vehicle selection and mission timelines. As with interplanetary mission design handbooks, an EDL mission design handbook could be constructed for each planet of interest.

The premise of this investigation is that Mars EDL can be parameterized with five variables: (1) entry mass, (2) entry velocity, (3) entry flight path angle, (4) vehicle aeroshell diameter, and (5) vertical lift-to-drag ratio. For combinations of these input parameters, the following trajectory information would be determined: peak deceleration, peak heat rate, total heat load, and the altitude at which Mach 2 is reached (for parachute deployment). The data would then be assembled and presented as a series of "pork chop" (contour) plots with the five EDL variables on the x and y axes and the trajectory information shown by the contours.

The central idea is that if a mission designer knows the entry conditions, size and aerodynamic properties for a particular planetary probe, the peak deceleration, peak heat rate, total heat load, and the altitude at which Mach 2 is reached for the trajectory can all be determined without having to run trajectory simulations. Similarly, the effects on the trajectory due to changes in the input parameters could quickly be determined. For example, the change in the Mach 2 altitude from an increase in entry mass could quickly be assessed.

2. METHODOLOGY

2.1 Major Variables

Ranges for the five parameters used to characterize Mars entry are shown in Table 1. The maximum value of the entry mass range was chosen based the expected entry mass for the Mars Science Lander (MSL) of approximately 2000 kg [1], which is currently the heaviest Martian planetary probe planned. The range of entry velocities and flight path angles were chosen to encompass the range of entry velocities seen by several successful probes, specifically for entry velocity: Viking 1 (4.61 km/s) [2] and Pathfinder (7.26 km/s) [3] and for entry flight path angle: Viking 2 (-17.027°) [2] and the Mars Exploration Rovers (MERs) (-11.5°) [4]. The range of aeroshell diameters bounds probes from Pathfinder (2.65 m) [3] to the largest probe which can pass through the environmental test chamber at the Jet Propulsion Laboratory (approximately 4.5 m allowing for handling equipment). The range of vertical lift-to-drag ratios encompasses ballistic entry (0) to a possible maximum value for blunt bodies (0.5).

Since both entry mass and aeroshell diameter are independent parameters in this investigation, a wide ballistic coefficient range is assessed as shown in Table 2. An alternative approach to this investigation might have been to use either entry mass or diameter as one independent variable and a packing density as the other variable. Packing density is a measure of how much mass could be put into an aeroshell of a given shape. The packing density could be used to determine either the aeroshell diameter for a given entry mass (by photographically scaling the aeroshell), or the entry mass for a given diameter of the aeroshell (by increasing the mass until the desired packing density was reached). The shaded ballistic coefficients in Table 2 show the range of values for a low packing density based on Viking and a high packing density based on MER.

Table 1: Ranges for the variables used to characterize Mars entry.

Input Parameter	Min	Max	Increment
Entry Mass (kg)	200	2000	200
Entry Velocity (km/s)	4	9	1
Entry Flight Path Angle (°)	-15	-10	0.5
Aeroshell Diameter (m)	2	5	1
Lift-to-Drag Ratio	0	0.5	0.1

Table 2: Ballistic coefficients based on entry mass and aeroshell diameter.

Ballistic Coefficient (kg/m²)		Diameter (m)			
		2	3	4	5
Mass (kg)	200	37.9	16.8	9.5	6.1
	400	75.8	33.7	18.9	12.1
	600	113.7	50.5	28.4	18.2
	800	151.6	67.4	37.9	24.3
	1000	189.5	84.2	47.4	30.3
	1200	227.4	101.1	56.8	36.4
	1400	265.3	117.9	66.3	42.4
	1600	303.2	134.7	75.8	48.5
	1800	341.0	151.6	85.3	54.6
	2000	378.9	168.4	94.7	60.6

Shaded values show the range of values for a low packing density based on Viking and a high packing density based on MER.

2.2 Commonalities between Trajectory Simulations

All 15,840 trajectories were simulated using the Program to Optimize Simulated Trajectories (POST) [5]. Each planetary probe was assumed to have a constant hypersonic drag coefficient of 1.68 [6] typical of 70° sphere-cone planetary probes. The vertical lift coefficient for the vehicle was determined by multiplying the drag coefficient with the vertical lift-to-drag ratio. For vehicles in banked flight, the lift coefficient would represent the portion of lift in the vertical direction.

All trajectory simulations used a common atmosphere. The atmospheric density on Mars varies significantly with time-of-year, time-of-day, dust-level (atmospheric opacity) and latitude. To account for the effects of each of these variables, a design atmospheric density profile was constructed from approximately one-thousand runs of Mars-GRAM 2005 [7] in which month, time of day, dust level, and latitude for the years of 2030 and 2031 were randomly varied. The results of the Mars-GRAM runs covered the range of densities shown in Fig. 1.

A cumulative distribution function of density was constructed for 0 km MOLA. The density at the 30% point on the 0 km cumulative distribution function (0.0124 kg/m³) as shown in Fig. 1 was chosen as the basis for the atmosphere. The atmosphere from the Mars-GRAM runs having a 0 km density of 0.0124 kg/m³ with the lowest 4 km density was then chosen for this investigation. The resulting atmosphere (shown in Fig. 2) was chosen for this investigation.

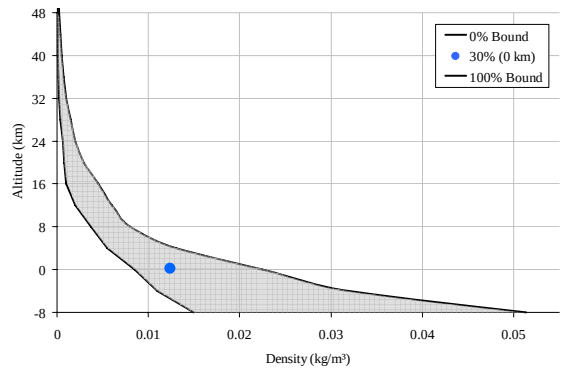

Fig. 1: The range of densities resulting from over 1000 runs of Mars-GRAM 2005.

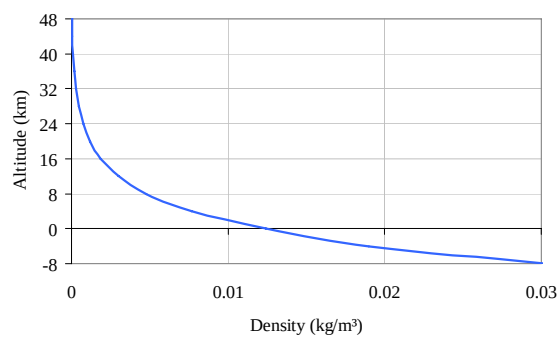

Fig. 2: Martian atmospheric density profile used for trajectory simulations.

2.3 Plots of Trajectory Data

After a trajectory for one combination of the input variables shown in Table 1 was run, the peak deceleration, peak heat rate, heat load, and Mach 2 altitude (for parachute deployment) were recorded. This data was then plotted against two of the major input variables (e.g. entry mass and flight path angle), while the other three major input variables (e.g. entry velocity, aeroshell diameter, and lift-to-drag ratio) were held constant. The data takes the form of contours in the plot such as that shown in Fig. 3 for peak deceleration.

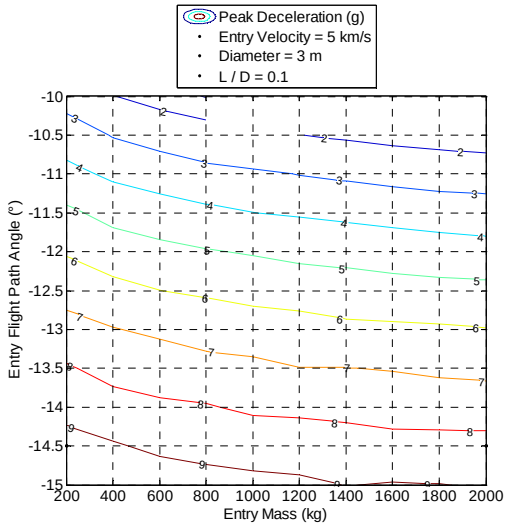

Fig. 3: An example plot of peak deceleration. The blank region between 800 and 2000 kg and -10° and -10.5° represents a region where the trajectory showed the probe skipping out of the atmosphere for a flight path angle of -10°, so contours cannot be plotted in this region.

Intersections of the gridlines on the contour plots show the specific points for which a trajectory simulation was run. Blank regions of the contour plots indicate combinations of major variables for which the simulations showed the probe skipping out of the atmosphere. Data was not recorded for cases which skipped out of the atmosphere. In order for contours to be plotted in any rectangular region bounded by the gridlines, the cases at the four vertices cannot have skipped out of the atmosphere, so contours cannot be plotted in these regions as shown in Fig. 4.

For example, in Fig. 3, the contour plot shows how peak deceleration varies with entry mass and flight path angle when entry velocity is held constant at 5 km/s, aeroshell diameter is held constant at 3 m, and the lift-to-drag ratio is held constant at 0.1. For this particular combination of entry velocity, aeroshell diameter, and flight path angle, the -10° flight path angle cases with masses from 1000 kg to 2000 kg skipped out of the atmosphere.

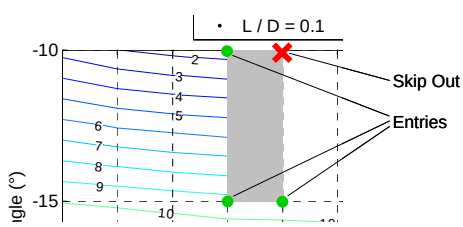

Fig. 4: Contour plots require successful entries for each of the four cases bounding regions of the plot.

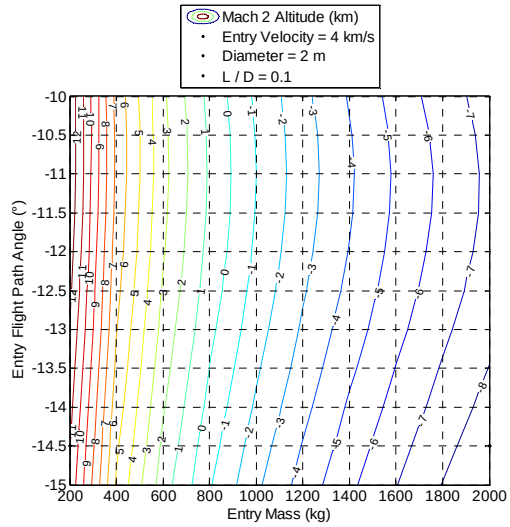

Fig. 5: An example plot of Mach 2 altitude. Mach 2 altitudes below -8 km were not plotted as the lowest point on Mars, located in Hellas Planitia, has an altitude of -8.18 km. [9]

The lowest point on Mars [9] has an elevation of -8.18 km, so Mach 2 altitudes lower than -8 km were not plotted on the contour plots as shown in Fig. 5.

3. RESULTS

The following paragraphs discuss some trends that can be seen in the results of the trajectory simulations. A sampling of the contour plots for peak deceleration, peak heat rate, heat load, and Mach 2 altitude are shown below. Note that plots were generally not made for combinations of variables which did not result in any successful entries (e.g. skip-out trajectories) that could be presented as a contour plot.

3.1 Peak Deceleration

As can be seen from Fig. 6, peak deceleration is generally not a strong function of entry mass when the entry velocity, aeroshell diameter, and lift-to-drag ratio are all fixed. Entry flight path angle, however, does significantly affect the peak deceleration of the entry trajectory when the other three major variables are fixed. Fig. 7 shows that peak deceleration is also a strong function of entry velocity in addition to entry flight path angle for a fixed entry mass, aeroshell diameter, and lift-to-drag ratio. However, for an entry flight path angle of approximately -12.7° in this investigation, peak deceleration is somewhat independent of entry velocity.

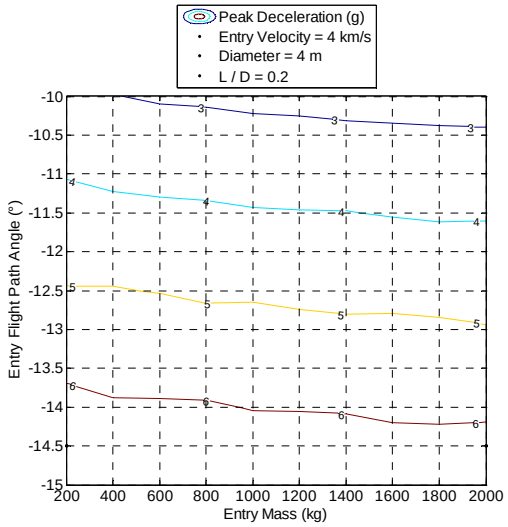

Fig. 6: Peak deceleration as a function of entry mass and flight path angle.

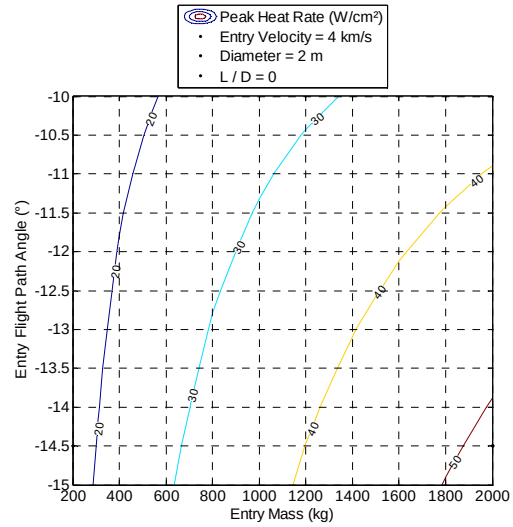

Fig. 8: Peak heat rate as a function of entry mass and flight path angle.

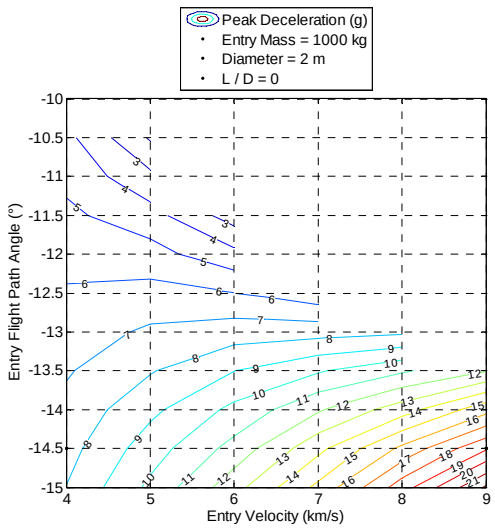

Fig. 7: Peak deceleration as a function of entry velocity and flight path angle.

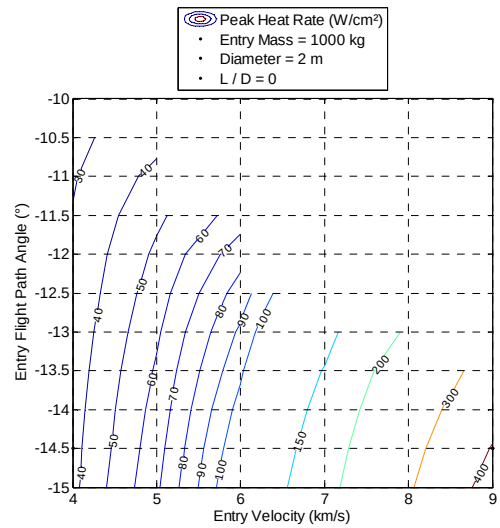

Fig. 9: Peak heat rate as a function of entry velocity and flight path angle.

3.2 Peak Heat Rate

The laminar stagnation point heat rate was calculated for each trajectory. Radiative effects were included for entry velocities above 6 km/s. [8] Peak heat rate increases with entry mass and slightly increases with entry flight path angle as shown in Fig. 8 for a fixed entry velocity, aeroshell diameter, and lift-to-drag ratio. Increasing entry velocity significantly increases peak heat rate as depicted in Fig. 9 for a fixed entry mass, aeroshell diameter, and lift-to-drag ratio. This is as expected since the major variables affecting heat rate are velocity, atmospheric density and the stagnation point radius.

3.3 Heat Load

Fig. 10 shows that heat load increases with entry mass and decreases with steepening of the entry flight path angle. As entry mass increases, heat load increases more quickly with entry mass at shallower entry flight path angles than at steeper flight path angles. Fig. 11 also shows that heat load increases with both entry velocity and shallower flight path angles, though more so with entry velocity, due to the higher heat rates experienced by the planetary probe, for a fixed entry mass, aeroshell diameter, and lift-to-drag ratio.

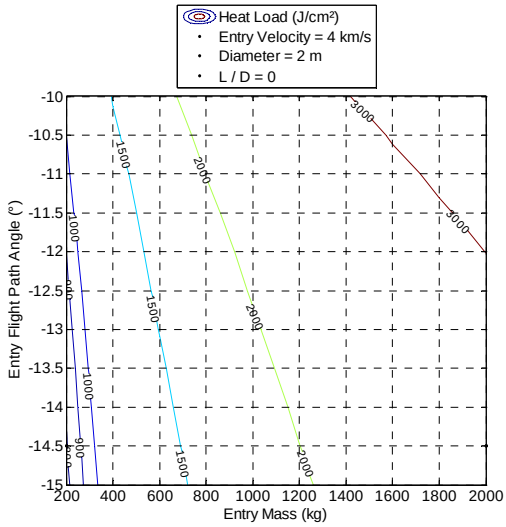

Fig. 10: Heat load as a function of entry mass and flight path angle.

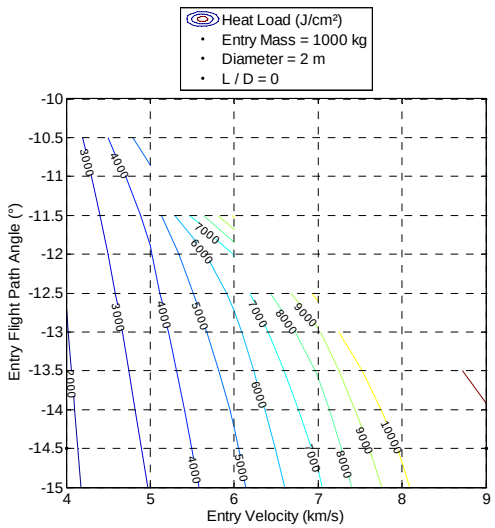

Fig. 11: Heat load as a function of entry velocity and flight path angle.

3.4 Mach 2 Altitude

Fig. 12 shows that the altitude at which Mach 2 is reached is strongly affected by the entry mass and less significantly affected by entry flight path angle when entry velocity, aeroshell diameter, and the lift-to-drag ratio of the planetary probe are all fixed. Fig. 13 also shows that the Mach 2 altitude generally increases as the aeroshell diameter of the probe increases. The larger diameter allows the planetary probe to slow down higher in the atmosphere and remain at a higher altitude when Mach 2 is reached.

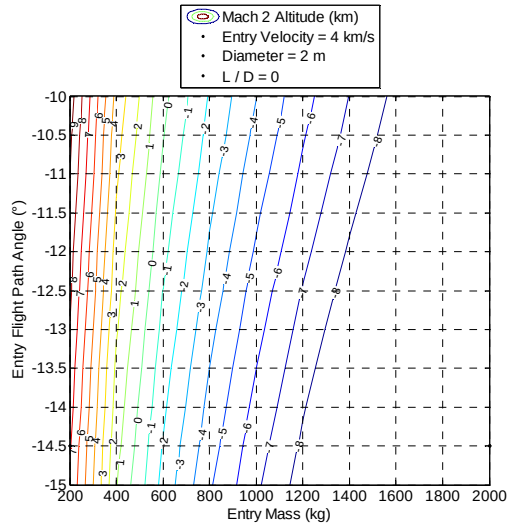

Fig. 12: Mach 2 altitude as a function of entry mass and flight path angle.

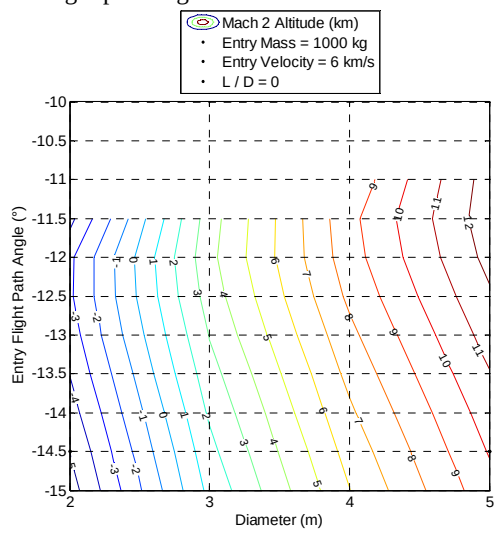

Fig. 13: Mach 2 altitude as a function of aeroshell diameter and entry flight path angle.

3.5 Conceptual Design

Once trajectory data has been compiled, as in this investigation, the data can be used to generate contour plots showing how design variables such as entry mass and lift-to-drag ratio can affect peak deceleration and peak heat rate. Table 3 lists design parameters for a conceptual Mars probe.

Table 3: Example parameters for a conceptual mission.

Parameter	Value
Entry Mass (kg)	200
Entry Velocity (km/s)	4
Entry Flight Path Angle (°)	-15
Aeroshell Diameter (m)	2
Lift-to-Drag Ratio	0

Contour plots specific to this conceptual mission, such as Fig. 14 and Fig. 15, show how changes in entry parameters can affect this conceptual mission. Note that the red dot in each figure represents the baseline mission. For example, Fig. 14 shows how increasing the flight path angle can impact peak deceleration, while Fig. 15 shows that changing the entry mass will affect the peak heat rate, but changing the lift-to-drag ratio in the vertical direction will not significantly change the peak heat rate.

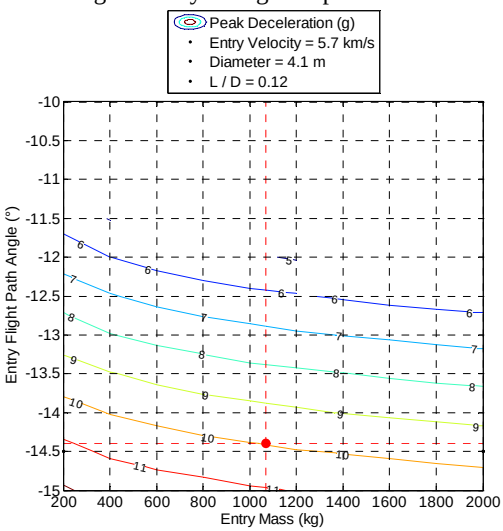

Fig. 14: How entry mass and flight path angle can impact the peak deceleration of a conceptual mission.

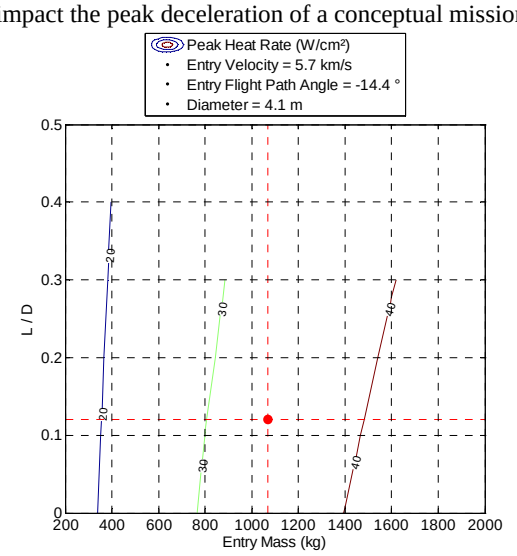

Fig. 15: How entry mass and lift-to-drag-ration can impact the peak heat rate of a conceptual mission.

4. CONCLUSIONS

Contour plots (or pork-chop plots as they are called by interplanetary mission designers) can be used to study trends in entry trajectories when major variables change. However, the number of independent major variables is more than can easily be represented in 2- or 3-dimensional plots, which makes looking at the effects of multiple variables difficult. Collections of contour plots such as those shown in this investigation can form the basis of entry mission design handbooks (the equivalent of interplanetary mission design handbooks). The contour plots in these handbooks can be general, or tailored to specific missions as shown in Fig. 14 and Fig. 15.

5. REFERENCES

1. Braun, R.D., Manning, R.M., "Mars Exploration Entry, Descent and Landing Challenges," *2006 IEEE Aerospace Conference*, IEEEAC paper #0076, Big Sky, Montana, March 2006.
2. Ingoldby, R. N., Michel, F. C., Flaherty, T. M., Doty, M. G., Preston, B., Villyard, K. W., Steele, R. D., "Entry Data Analysis for Viking Landers 1 and 2 Final Report", Martin Marietta Corp., NASA TN 3770218, NASA CR 159388, November 1976.
3. Spencer, D.A., Blanchard, R.C., Braun, R.D., Kallemeyn, P.H., Thurman, S.W., "Mars Pathfinder Entry, Descent, and Landing Reconstruction", *Journal of Spacecraft and Rockets*, Vol. 36, No. 3, May-June 1999.
4. Desai, P.N., Knocke, P.C., "Mars Exploration Rovers Entry, Descent, and Landing Trajectory Analysis," *AIAA/AAS Astrodynamics Specialist Conference and Exhibit*, AIAA-2004-5092, Providence, Rhode Island, August 16-19, 2004.
5. POST, Program to Optimize Simulated Trajectories, Ver. 5.2, NASA Langley Research Center, Hampton, Virginia, Martin Marietta Corporation, Denver, Colorado, 1997.
6. Gnoffo, P., Braun, R.D., Weilmuenster, K.J., Mitcheltree, R.A., Engelund, W.C., Powell, R.W., "Prediction and Validation of Mars Pathfinder Hypersonic Aerodynamic Database," *7th AIAA/ASME Joint Thermophysics and Heat Transfer Conference*, AIAA-1998-2445, Albuquerque, New Mexico, June 1998.
7. Mars-GRAM, Mars Global Reference Atmospheric Model, Ver 2005, Computer Sciences Corporation, Huntsville Alabama, NASA Marshall Spaceflight Center, Alabama, 2005.
8. Tauber, M.E., Sutton, K., "Stagnation-Point Radiative Heating Relations for Earth and Mars Entries", *Journal of Spacecraft and Rockets*, Vol. 28, pp. 40-42, January-February 1991.
9. Mars, The Red Planet Reference Map," Copyright © 2001 *National Geographic Society*, Washington, DC.